FIZIKA, 8 (1976) 87—97

X-RAY DIFFRACTION STUDY OF SPLAT-QUENCHED Ag-6 at. % Sn AND Ag-11 at. % Sn ALLOY

A. M. TONEJC, A. KIRIN and A. BONEFAČIĆ

Institute of Physics of the University, Zagreb

Received 17 February 1976

Abstract: An analysis of X-ray powder pattern peaks of splat quenched Ag-6 at. % Sn and Ag-11 at. % Sn alloy was used in order to determine microstrains, effective particle sizes and deformation and twin stacking fault probabilities. The shapes and positions of all available (hkl) reflections for Cu K_α radiation were recorded, using focusing Bragg-Brentano X-ray geometry. Fourier analysis was performed on the profiles of 111—222 and 200—400 pairs of reflections. The effective particle sizes D_{e111} and D_{e100} decreased and microstrains increased with increasing solute concentration. During isochronal annealing, the temperature of the beginning of recovery in different samples showed to be dependent on the tin concentration which influenced the microstrains and the effective particle size variations during annealing. The deformation fault and twin fault probabilities were found to be low and of about equal value. The stacking fault energy was also determined for both examined alloys. The particle sizes, microstrains, fault probabilities and fault energies were compared with correspondent values obtained for cold-worked filings and for deformed in compression and subsequently annealed bulk alloys in the same domain of Sn concentrations.

1. Introduction

A great deal of experimental work on splat cooling techniques has been reported (e. g. Ref.[1]) over the last ten years, but except for some papers[2,3,4,5], little attention has been given to the microstructure of rapidly quenched samples.

By rapid quenching from the melt a high concentration of defects may be quenched-in[6], solid solubility may be extended over the equilibrium values[7],

and if the two-piston quenching technique[8] is used, it is not difficult to imagine that quenched samples may become plastically deformed to an unknown degree during quenching. Namely, droplets of liquid alloy, ejected between two rapidly moving pistons, are not only squeezed between them, but, after completed solidification, solid samples may undergo a certain plastic deformation caused by the shock of the pistons in collision.

The purpose of the present work was to investigate the microstructure of an alloy, quenched by the two-piston method, as regards crystallite size, lattice strains and lattice stacking faults. Line broadening analysis of diffraction patterns and shifts in the position of diffraction peaks was made using the method of Warren[9].

Ag-rich Ag-Sn alloys were chosen for the experimental work for the following reasons: as previously shown, faulting occurs when this material is filed[10,11], or deformed in compression[12]. Since Ag and Sn have roughly the same scattering factor, the Suzuki effect[13] is minimized.

Two alloy compositions were used in the present experiments: Ag-6 at. % Sn and Ag-11 at. % Sn (with notations Ag6Sn and Ag11Sn). Ag6Sn is an equilibrium α-Ag fcc solid solution, while the composition of Ag11Sn represents the limit of the solid solubility of Sn in Ag at 600°C[14].

2. *Experimental procedure*

Silver-tin alloys were prepared from spectrographically standardized silver and tin. Accurately weighed quantities of the metal components were melted together in evacuated and sealed quartz capsules. During the melting, the capsules were shaken. After melting, the alloys were homogenized for one day at a temperature of 800 °C and furnace-cooled. Weight changes during preparation were negligible. The ingots were rapidly quenched from the melt by the two-piston method[8] from a temperature of about 1200 °C. Quenched flakes of equal thickness, or one large flake, were stuck on to a pyrex substrate and examined by X-ray diffraction analysis. The sample thickness used in the experiments was about 30 μm.

Diffraction line profiles were studied on a Siemens diffractometer with a step scanning device using Bragg-Brentano focusing geometry, as reported previously[4]. Radiation was monochromated with a bent quartz crystal, which focused the Cu K_α radiation on the entrance slit of the counter. A scintillation counter was used with a single channel pulse height analyser. The experimental conditions included the use of an 0.7° divergence slit and an 0.1 mm receiving slit. To avoid the influence of preferred orientation of crystallites on distribution intensity, an oscillating attachement was used, with an oscillation frequency of 1 s^{-1}.

Fourier analysis of line broadening was preferred to integral breadth analysis, since the former yields more details about microstrain distribution, and no

assumption is required regarding the shapes of peaks. The Fourier coefficients of the line profiles of the quenched samples were corrected for instrumental broadening by the Stokes method[15], using the same but well annealed sample as a standard. The isochronal annealing procedure was used for annealing. Separate specimens of each of the two alloys were annealed in vacuum for 15 minutes at different temperatures (from 25°C to 500°C).

For recording the obtained line profiles, 127 readings on 1° were taken which gives a total of about 250 readings for line 111 and about 600 readings for line 400. Fourier analysis of the broadened peaks, and the Stokes correction for instrumental broadening were made using a computer program written in Fortran.

3. *Fourier analysis of line broadening*

In the present work the method developed by Warren and Averbach[16], Warren[9], and Halder and Wagner[17] was applied in order to analyse the broadening of powder patterns. The details can also be found in Refs.[18, 19, 20, 21], and so only a brief description will be given here.

The profile of a powder pattern peak corrected for instrumental broadening can be expressed in terms of a Fourier series[9]

$$P(2\Theta) = K \sum_n \{A(L) \cos [4\pi L (\sin\Theta - \sin\Theta_0)/\lambda] + B(L) \sin [4\pi L (\sin\Theta - \sin\Theta_0)/\lambda]\}, \quad (1)$$

where K is the constant, $L = nd_{hkl}$ the distance normal to the reflecting planes (hkl) of interplanar spacings d_{hkl}, Θ_0 the position of the peak maximum, and λ the wave length of the radiation.

The Fourier coefficients $A(L)$ can be written as[21]

$$A(L) = A^P(L) \quad A^\varepsilon(L), \quad (2)$$

where the peak maximum is used as the origin of the Fourier integral and the superscripts P and ε represent the particle size and strain component of each coefficient.

$A^P(L)$ and $A^\varepsilon(L)$ can be approximated for small values of L as

$$A^P(L) = 1 - \frac{L}{D_{ehkl}} = 1 - L\left(\frac{1}{D} + \frac{1.5\,\alpha + \beta}{a} V_{hkl}\right) \quad (3)$$

$$A^\varepsilon(L) = 1 - 2\pi^2 L^2 \langle \varepsilon_L^2 \rangle_{hkl} \frac{h_0^2}{a^2},$$

where $\langle \varepsilon_L^2 \rangle_{hkl}$ is the mean square strain (MSS) component normal to the reflecting planes (hkl). D_{ehkl} is the effective particle size, D is the true particle size, α the deformation stacking fault probability, β the twin stacking fault probability, $h_0^2 = h^2 + k^2 + l^2$, and a the lattice parameter. V_{hkl} is constant for a given direction and can be found in Ref.[20]. Some of the values are: $V_{111} = 0.43$, $V_{200} = 1$, $V_{220} = 0.71$.

The Warren and Averbach method[16] was used to separate the strain term $A^e(L)$, which is h_0^2 dependent, from the independent particle size term $A^P(L)$. In this case $A(L)$ can be expressed as

$$\ln A(L) = \ln A^P(L) - 2\pi^2 L^2 \langle \varepsilon_L^2 \rangle_{hkl} \frac{h_0^2}{a^2}. \tag{5}$$

Plot $\ln A(L)$ vs h_0^2 with extrapolation to $h_0^2 = 0$ gives the particle size coefficient $A^P(L)$ for different values of L. The slopes give the MSS $\langle \varepsilon_L^2 \rangle_{hkl}$ for different L, and $[\langle \varepsilon_L^2 \rangle_{hkl}]^{1/2}$ is the root mean square strain (RMSS) of the strain distribution. By plotting $A^P(L)$ vs L and taking the intercept of the initial slope with the abscissa L, the effective particle size D_{ehkl} for $\langle hkl \rangle$ directions can be obtained. Obtaining the numerical values of D_{e111} and D_{e100}, and using relation (3), the values of the domain sizes D and faulting probability term $(1.5\,\alpha + \beta)$ can be determined.

The stacking fault probability α was determined from the shift in the diffraction peak positions ($\Delta\Delta 2\Theta$) on the as-quenched (as q.) and annealed (ann.) reference specimen, according to the relation[9]

$$\alpha = \frac{(2\Theta_{200} - 2\Theta_{111})\ \text{as q.} - (2\Theta_{200} - 2\Theta_{111})\ \text{ann.}}{-45\sqrt{3}/\pi^2 \left(\tan\Theta_{200} + \frac{1}{2}\tan\Theta_{111}\right)}, \tag{6}$$

or

$$\alpha = (-0.1266)\ \Delta\Delta 2\Theta / (\tan 2\Theta_{200} + \frac{1}{2}\tan\Theta_{111}). \tag{7}$$

4. *Experimental results*

The experimental results obtained on splat-quenched samples of two Ag-Sn alloys, Ag6Sn and Ag11Sn, are presented. Both alloys were α-Ag fcc solid solutions which was confirmed by comparing their lattice parameters with the results published by Klement[22].

RMSS were measured in the [111] and [100] directions, and in all as-quenched samples the value of RMSS decreased asymptotically with increasing L (e.

g. Fig. 1), with a very pronounced initial drop of up to $L = 100$ Å. We can see that the decrease of RMSS is fairly rapid in the initial range of temperatures and that it reaches a constant value at about 200 °C for Ag6Sn (Fig. 2). A similar slope was found for the Ag11Sn alloy, and the constant value of RMSS was obtained at about 350 °C. The annealed values of RMSS are smaller by a factor of about two in comparison with the values obtained from the as-quenched samples.

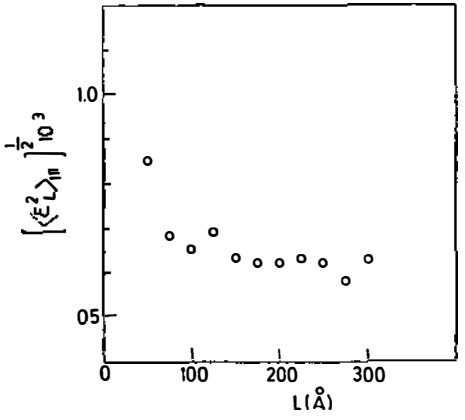

Fig. 1. The plot of $[\langle\varepsilon_L^2\rangle_{111}]^{\frac{1}{2}}$ versus distance $L = nd_{111}$ for as-quenched Ag6Sn alloy.

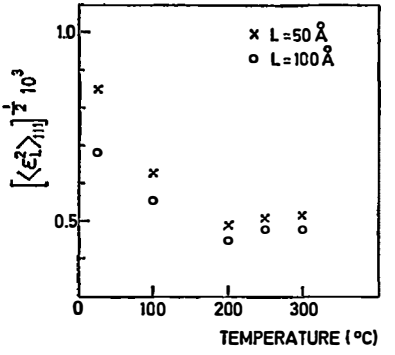

Fig. 2. Values of $[\langle\varepsilon_L^2\rangle_{111}]^{\frac{1}{2}}$ as a function of annealing temperature for Ag6Sn splat cooled sample.

The effective particle sizes D_{chkl} in the [111] and [100] directions were obtained by measuring the intercept of the initial slope of the strain-corrected Fourier coefficients $A^P(L)$ with the abscissa L. The effective particle sizes D_{chkl} as functions of the annealing temperature are represented in Fig. 3. We can see that the effective domain sizes in the [111] direction are larger for smaller concentrations of solute. It is also evident that the effective grain size in Ag6Sn as-quenched alloys begins to grow at approximately 100 °C, while in Ag11Sn this takes place at temperatures exceeding 200 °C.

Particle sizes and strains in splat-quenched Ag6Sn and Ag11Sn samples are given in Table 1.

TABLE 1.

Particle sizes and strains in splat-quenched Ag6Sn and Ag11Sn.

Variable / Alloy	$[\langle\varepsilon_{30}^2\rangle_{111}]^{\frac{1}{2}}$	$[\langle\varepsilon_{30}^2\rangle_{100}]^{\frac{1}{2}}$	D_{c111}(Å)	D_{c100}(Å)	D_{c311}(Å)	D_{c220}(Å)	D (Å)
Ag6Sn	$0.85 \cdot 10^{-3}$	$1.06 \cdot 10^{-3}$	1200	900	720	880	1350
Ag11Sn	$1.44 \cdot 10^{-3}$	$2.34 \cdot 10^{-3}$	700	510	580	550	1100

The stacking fault probability α (using relation (7)) was calculated only for as-quenched samples. After annealing at higher temperatures, the shift of the line peak ($\Delta\Delta 2\Theta$) was too small to be distinguished from the error in determining the peak position.

Since it is possible to anneal out a certain proportion c of Sn ($c < 0.5$ at.% Sn 500 °C) from the Ag11Sn solid solution (see phase diagram Ag-Sn[14]), one should see how this effect may influence the measurements of α. A simple calculation shows that annealing out 0.5 at. % Sn (which is the most unfavourable case) causes a change of about 0.004° in $(\Delta\Delta 2\Theta)^{*}_{111-200}$. It is very easy to show that this change has a tendency to increase the difference $(\Delta\Delta 2\Theta)^{s.f.}_{111-200}$ due to stacking faults (s. f.). If the measured value $(\Delta\Delta 2\Theta)^{s.f.}_{111-200}$, greatly exceeds $(\Delta\Delta 2\Theta)^{*}_{111-200}$, the latter may be neglected. On the contrary, if it is too large to be neglected, the measured value of $(\Delta\Delta 2\Theta)^{s.f.}_{111-200}$ must be reduced by this value in order to obtain the real $(\Delta\Delta 2\Theta)^{s.f.}_{111-200}$.

In our case $(\Delta\Delta 2\Theta)^{s.f.}_{111-200}$ was 0.023°, and in our calculations we neglected the term $(\Delta\Delta 2\Theta)^{*}_{111-200}$.

The α-values of as-quenched Ag6Sn and Ag11Sn samples are given in Table 4.

5. *Discussion*

Microscopic strains. In as-quenched samples the RMSS values $[\langle\varepsilon_L^2\rangle_{hkl}]^{1/2}$ (for $L = 50$ Å) for Ag11Sn were about twice the value for Ag6Sn (precisely a ratio of 2.3 for the [100] and 1.7 for the [111] direction). This is in accordance with previous results on filings[10,11] where a gradual increase was found in RMSS

TABLE 2.

Microstrains $[\langle\varepsilon_{50}^2\rangle_{hkl}]^{\frac{1}{2}} \cdot 10^3$ for directions [111] and [100].

	Filings[10]	Filings[11]	RCA[12]	Splat-quenched
Ag6Sn [111]	3.8	3.1		0.85
Ag6Sn [100]	5.5			1.06
Ag9Sn [111]	4.6	3.6	1.2	
Ag11Sn [111]				1.44
Ag11Sn [100]				2.34

values in the [111] and [100] directions as the Sn content was increased. The values for RMSS in the [100] direction were also found to be greater than those in the [111] direction as found in the present work (Table 2).

On an absolute scale the RMSS values obtained on filings[10,11] were about five times greater than the values obtained on as-quenched samples for the same Sn content (6 at. %). This, and the fact that for the same alloy composition (6 at. %) the filings have a much higher value of deformation fault probability ($23 \cdot 10^{-3}$ as against $3 \cdot 10^{-3}$ in as-quenched samples) suggests that in filings in comparison to as-quenched samples there exists a higher density of dislocations. However, our RMSS values are very comparable to the RMSS values found in bulk specimens, which were plastically deformed by compression and annealed for 1 hr at 390 °C[12] (in Table 2 these samples are denoted RCA).

TABLE 3.

Effective particle sizes D_{ehkl} (Å) in directions [111] and [100].

	Filings[10]	Filings[11]	RCA[12]	Splat-quenched
Ag6Sn [111]	135	170		1200
Ag6Sn [100]	75			900
Ag9Sn [111]	71	150	600	
Ag9Sn [100]	37		240	
Ag11Sn [111]				770
Ag11Sn [100]				510

The ratio between $RMSS_{100}$ and $RMSS_{111}$ is about 1.4 for Ag6Sn filings[10], 1.3 for Ag6Sn, and 1.6 for Ag11Sn splat quenched samples. For an ideal isotropic stress model, according to which the residual microstrains in the ⟨hkl⟩ directions will be inversely proportional to Young's modulus E_{hkl}, the anisotropy strain ratio E_{111}/E_{100} would be 3.0 for Ag6Sn and 3.1 for Ag11Sn (in our calculations we used published elastic constants for Ag and Ag-3.17 at. % Sn alloy[23] and extrapolated them to 6 and 11 at. % tin). For ideal isotropic strains this ratio would be 1. The anisotropy of measured RMSS in as-quenched samples suggests the existence of a non-uniform distribution of dislocations and stacking faults.

Particle sizes. The effective particle sizes measured in the [111] and [100] directions are anisotropic because D_{e111}/D_{e100} is greater than unity. If the stacking faults (either deformation or twin stacking faults) are entirely responsible for the anisotropy of D_{ehkl}, then the theoretical ratio will be 2.3, and the effect of the true particle size may be neglected[10]. Allowing for experimental uncertainty, this is nearly the case with filings where the ratio is about 1.9, and with RCA samples where the ratio is slightly greater[12]. This closer agreement with the theoretical ratio would mean that the anisotropy of the effective particle sizes D_{ehkl} is mainly a consequence of faulting in the samples. The lower ratio (about 1.5) in as-quenched samples suggests that the true particle sizes also influence both the magnitude of the measured effective particle sizes and the faulting.

Here again the D_{ehkl} values of as-quenched samples compare much better with RCA samples (Table 3) than with filings. In all three cases (filings, RCA, and as-quenched samples) the D_{ehkl} values decrease with increasing Sn content. However, the true crystallite size D does not seem to be greatly influenced by the Sn concentration in as-quenched samples, and its value is of the order of crystallite size as seen by electron microscope (700—1000 Å)[24].

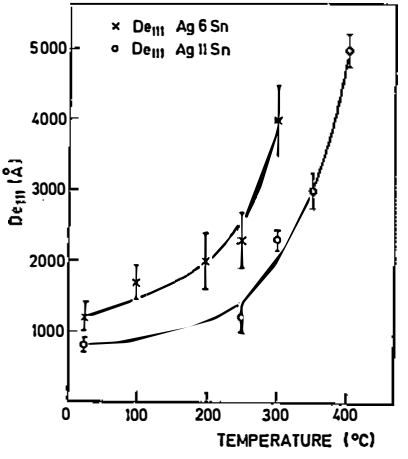

Fig. 3. Isochronal annealing of the effective domain sizes D_{e111} with temperature for Ag6Sn (×) and Ag11Sn (o).

In Fig. 3 we can see that the temperature of recovery of the effective domain size increases with increasing solute concentration, an effect which was also observed in filings[11].

Stacking fault probability and energy. Table 4 gives the values of α, calculated using relation (7), while relation (3) gives the possibility to obtain some information on eventually existing twin faults. Inserting the independent calculated α values into the relation[12]

$$1.5\alpha + \beta = \frac{a}{V_{111}} \cdot \frac{1}{D_{e111}}, \tag{8}$$

we shall obtain the twin fault probability β. (Table 4).

TABLE 4.
Deformation fault probability α, twin fault probability β and stacking fault energy γ in splat-quenched Ag6Sn and Ag11Sn.

	α	β	γ (mJ/m²)
Ag6Sn	0.003	0.004	1.88
Ag11Sn	0.006	0.004	2.61

For both examined alloys (Ag6Sn and Ag11Sn) the obtained β values were the same (equal to 0.004). Comparing β with α, we shall see that there exists about the same probability that twinning and deformation stacking faults exist in as--quenched samples.

The twin fault probability β in filings is very high ($\approx 18 \cdot 10^{-3}$ for Ag6Sn[10]), however no twin fault has been found in RCA samples[12] with a crystallite size of 30—50 μm, while in RCA samples, with a smaller crystallite size (5—10 μm), a twin probability was found ($\beta \approx 3 \cdot 10^{-3}$)[12] which also indicated the possibility of finding twins in splat-quenched samples because of the smaller size of the crystallites.

This theoretical prediction of twinning is in agreement with the result obtained by electron microscopy[24] where twin faults were observed in both Ag6Sn and Ag11Sn splat cooled as-quenched samples. The values for RCA samples ($\alpha = 0.003$ and $\beta = 0.004$)[12] are very comparable with the values obtained on splat--quenched samples in our own experiments.

The stacking fault energy γ was calculated using the relation proposed by Reed and Schramm[25]

$$\gamma = \frac{K_{111}\,\omega_0\,G_{(111)}\,a}{\pi\sqrt{3}}\,A^{-0.37}\,\frac{\langle \varepsilon_{50}^2 \rangle_{111}}{a}, \tag{9}$$

where $K_{111}\,\omega_0 = 6.6$, $G_{(111)}$ is the shear modulus in the (111) fault plane and equals $\frac{1}{3}(c_{44} + c_{11} - c_{12})$, a is the lattice parameter and $A = \frac{2c_{44}}{c_{11} - c_{12}} \cdot c_{ij}$ are elastic stiffness coefficients, given in Ref.[23].

Reed and Schramm[25] have noted that because of strong dependence of the values of both microstrain and stacking fault probabilities on the degree of plastic deformation, both quantities must be measured on the same specimen at the same time. This was the case in our experiments. Ruff and Ives[26] showed that γ-values obtained in Ag9Sn alloy depend on the history of specimens. Depending on whether the specimens were as-deformed, bulk annealed, foil annealed or quenched, they obtained values for γ between 0.8 and 3.4 mJ/m^2. We can state that γ--values in our samples, which were both deformed and quenched, can be included in Ruff and Ives's interval of γ-values.

6. *Summary*

The broadening and shift of X-ray diffraction peaks from splat quenched Ag-6 at. % Sn and Ag-11 at. % Sn were studied. The Fourier analysis was used for separating the broadening due to the small effective particle size and to microstrains. The following conclusions were drawn:

X-ray line broadening was found to be due to microstrains, stacking faults, and the reduction of the size of coherently diffracting domains.

Microstrains increased and effective domain sizes decreased with increasing solute concentration.

Isochronal annealing studies showed that higher temperatures are needed for the recovery of microstrains and effective domain sizes when the solute concentration increases.

No significant difference in stacking fault probability was found for different contents of Sn in the samples. Equal probability of deformation and twin stacking faults was estimated.

The established values of stacking fault energies are consistent with published values.

Splat-quenched Ag-Sn alloys showed about one order of magnitude lower value of microstrains, deformation and twin fault probability than are those found in filings. Howerer those values were very similar to the values of annealed bulk samples obtained by reduction-compression.

Acknowledgements

The authors wish to thank Dr. A. Tonejc for providing the samples and to Dr. J. Dixmier, Faculté des Science, Orsay, for giving the opportunity to carry out the final computer calculations.

References

1) H. Jones and C. Suryanarayana, J. Mat. Sci. **8** (1973) 705;
2) P. Furrer, T. R. Anantharaman and H. Warlimont, Phil. Mag. **21** (1970) 873;
3) P. Ramachandrarao, P. R. Rao and T. R. Anantharaman, Z. Metallk. **61** (1970) 471;
4) A. Kirin and A. Bonefačić, J. Phys. F **4** (1974) 1608;
5) R. B. Roof and R. O. Elliot, J. Mat. Sci. **10** (1975) 101;
6) G. Thomas and R. H. Willens, Acta Met. **12** (1964) 191;
7) T. R. Anantharaman and C. Suryanarayana, J. Mat. Sci. **6** (1971) 111;
8) J. Dixmier and A. Guinier, Mém. Scient. Rev. Métall. **64** (1967) 53;
9) B. E. Warren, Progress Met. Phys. **8** (1959) 147;
10) R. P. I. Adler and C. N. J. Wagner, J. Appl. Phys. **33** (1962) 3451;
11) C. J. Newton and A. W. Ruff Jr., Met. Trans. **1** (1970) 2833;
12) R. P. I. Adler and C. N. J. Wagner, Met. Trans. **1** (1970) 2791;
13) J. P. Hirth, Met. Trans. **1** (1970) 2367;
14) M. Hansen, Constitution of Binary Alloys, McGraw-Hill Book Comp., London, 1958., p. 53;
15) A. R. Stokes, Proc. Phys. Soc. London, **61** (1948) 382;
16) B. E. Warren and B. L. Averbach, J. Appl. Phys. **21** (1950) 595;
17) N. C. Halder and C. N. J. Wagner, Adv. X-Ray Analysis, **9** (1966) 91;
18) B. E. Warren and B. L. Averbach, J. Appl. Phys. **23** (1952) 497;
19) C. N. J. Wagner, A. S. Tetelman and H. M. Otte, J. Appl. Phys. **33** (1962) 3080;

20) B. E. Warren, X-Ray Diffraction, Addison-Wesley, Reading, Massachusetts, 1969. p. 251 —298;
21) C. N. J. Wagner, Local Atomic Arrangements Studied by X-Ray Diffraction, Gordon and Breach, New York 1966., p. 219;
22) W. Klement Jr., Trans. AIME **233** (1965) 1182;
23) G. Simmons and H. Wang, Single Crystals Elastic Constants and Calculated Aggregate Properties: A Handbook, The M. I. T. Press, London, 1971., p. 86 and 90;
24) A. M. Tonejc, D. Kunstelj and A. Bonefačić, Proc. Yug. Centre of Crystallography, **10** (1975);
25) R. P. Reed and R. E. Schramm, J. Appl. Phys. **45** (1974) 4705;
26) A. W. Ruff and L. K. Ives, Phys. Stat. Sol. (a) **16** (1973) 133.

PROUČAVANJE MIKROSTRUKTURNIH SVOJSTAVA ULTRABRZO KALJENIH Ag-6 at. % Sn I Ag-11 at. % Sn SLITINA POMOĆU RENDGENSKE DIFRAKCIJE

A. M. TONEJC, A. KIRIN i A. BONEFAČIĆ

Institut za fiziku Sveučilišta, Zagreb

Sadržaj

Pomoću rendgenske difrakcije analizirani su uzorci ultrabrzo kaljenih Ag-6 at. % Sn i Ag-11 at. % Sn slitina da bi se odredili mikrostrukturni parametri: mikronaprezanje, veličina zrna, vjerojatnost pogrešaka u slaganju nastalih deformacijom i sraštanjem. Oblik i položaj svih difrakcijskih refleksa, dobivenih Cu K_α zračenjem, registrirani su pomoću Bragg-Brentano difrakcijske geometrije.

Fourierova analiza provedena je na profilima parova linija 111—222 i 200 —400. Efektivne veličine zrna D_{e111} i D_{e100} opadaju, a mikronapetosti rastu s povećanjem kositra u uzorcima.

Tijekom izohronog popuštanja temperatura pri kojoj započinje oporavak zavisna je o koncentraciji kositra u uzorcima, što utječe kako na mikronapetosti, tako i na efektivne veličine zrna. Pogreške slaganja prouzrokovane sraštanjem i deformacijom podjednako su vjerojatne. Izračunata je energija pogrešaka u slaganju.

Sve mjerene veličine uspoređene su s ranije objavljenim rezultatima dobivenim na strugotinama slitina Ag-Sn istih koncentracija, kao i na masivnim uzorcima slitina Ag-Sn koje su bile deformirane i toplinski obrađivane.